Molecular Crystals and Liquid Crystals
Publication details, including instructions for authors and subscription information:
http://www.tandfonline.com/loi/gmcl20

Polymer Material Dependence in the Polymer/Small Molecule Metal-Base Organic Transistors

K. Umetsu [a], R. Akiba [a], K. Nakayama [a b] & J. Kido [a b]
[a] Department of Organic Device Engineering, Yamagata University, Yonezawa, Yamagata, Japan
[b] Research Center for Organic Electronics, Yonezawa, Yamagata, Japan
Published online: 11 Sep 2013.

To cite this article: K. Umetsu, R. Akiba, K. Nakayama & J. Kido (2013) Polymer Material Dependence in the Polymer/Small Molecule Metal-Base Organic Transistors, Molecular Crystals and Liquid Crystals, 580:1, 117-124, DOI: 10.1080/15421406.2013.808119

To link to this article: http://dx.doi.org/10.1080/15421406.2013.808119

Mol. Cryst. Liq. Cryst., Vol. 580: pp. 117–124, 2013

ISSN: 1542-1406 print/1563-5287 online
DOI: 10.1080/15421406.2013.808119

Taylor & Francis
Taylor & Francis Group

Polymer Material Dependence in the Polymer/Small Molecule Metal-Base Organic Transistors

K. UMETSU,[1] R. AKIBA,[1] K. NAKAYAMA,[1,2,*] AND J. KIDO[1,2]

[1]Department of Organic Device Engineering, Yamagata University, Yonezawa, Yamagata, Japan
[2]Research Center for Organic Electronics, Yonezawa, Yamagata, Japan

A hybrid metal-base organic transistor composed of a vacuum-deposited small-molecule emitter layer and a solution-processed polymer collector layer was fabricated using three types of conductive polymer, poly(3-hexylthiophene) (P3HT), poly(2-methoxy-5(2′-ethyl)hexoxy-phenylenevinylene (MEH-PPV) and poly(9, 9-dioctylfluorene-co-benzothiadiazole) (F8BT). Clear current amplification was observed only in the device with P3HT, and output current density of 12.6 mA/cm^2, on/off ratio of 10^5, and current amplification factor of 76 were achieved at a collector voltage of 5 V and base voltage of 3 V. The output current decreased in order of P3HT > MEH-PPV > F8BT. The relationship between energy levels of polymer materials and carrier transmission process through the base electrode were discussed.

Keywords Energy level; metal-base organic transistors; polymer; solution-process

Introduction

Organic thin-film transistors have been studied extensively due to the advantages of low temperature fabrication, low production cost, and flexibility. They are expected to be used for various applications such as flexible integrated circuits, displays [1–2], and radio frequency identification tags [3–4]. Organic thin-film transistors usually mean organic field effect transistors (OFETs) having a lateral channel where the device performance is improved by reducing the channel length, as in silicon FET devices. However, it is difficult to reduce the channel length less than 10 microns without using expensive lithography techniques. As a different approach to solve this problem, several types of organic transistors having vertical channel have been proposed, such as organic static-induction transistors (OSIT) [5–7], space-charge limited transistors (SCLT) [8–10], polymer hot-career transistor [11–12], and organic triodes [13–17]. In these devices, channel length can be easily reduced to less than 1 μm because it corresponds to the thickness of the organic layer. Our proposed metal-base organic transistor (MBOT) [18–21] is a high performance vertical organic transistor with a simple organic/metal/organic layered structure. The MBOT exhibits current amplification similar to silicon bipolar transistors, and large output current modulation exceeding 100 mA/cm^2 at low operation voltage of several volts.

Thus far, transistor behavior in the MBOT has been observed in only n-type material such as perylene bisimide compounds and fullerene, and its fabrication process has been

*Address correspondence to Ken-ichi Nakayama, Yamagata University, 4-3-16 Jonan, Yonezawa, Yamagata 992-8510, Japan. Tel./Fax: +81-238-26-3713; E-mail: nakayama@yz.yamagata-u.ac.jp.

limited to vacuum deposition. Very recently, however, we have reported a high performance p-type MBOT using a very common material of pentacene [22]. This achievement opened up the door to explore various kinds of materials including polymers in the MBOT. In this study, we fabricated a hybrid MBOT composed of vacuum deposited emitter layer and solution-processed collector layer. Three types of conductive polymer, P3HT, MEH-PPV and F8BT, were employed and compared. From the device performance, we discussed selection guide of materials for current amplification in the p-type MBOTs.

Experiment

The hybrid MBOT was fabricated by spin-coating of polymer layer and vacuum deposition of small molecule on indium tin oxide (ITO) glass substrates. The device structures and molecule structures of employed three types of polymers (P3HT, MEH-PPV and F8BT) are shown in Fig. 1. These polymer materials were supplied from Lumtec, and each molecular weight of P3HT, MEH-PPV and F8BT was 80,000 $\sim$ 90,000, 500,000 $\sim$ 1,000,000 and 20,000 $\sim$ 50,000, respectively. The polymer with a thickness of 200 nm was prepared on a cleaned ITO glass substrate by spin-coating as the collector layer. After deposition of LiF(1.6 nm)/Al(10 nm) layers, the substrate was subjected to a heat treatment for one hour at 100°C under atmospheric condition. After deposition of a thin LiF layer (3 nm), the emitter layer of CuPc (100 nm) and the top MoO_3 (2 nm)/Au(30 nm) emitter electrode were also evaporated thermally. The ITO electrode, LiF/Al/LiF layers, and MoO_3/Au layers are the collector electrode, base electrode, and emitter electrode, respectively.

The vacuum chamber was flushed with dry nitrogen gas, and the device was immediately transferred to a glove box system to reduce the effect of atmospheric exposure. The size of the active area in which the three electrodes overlapped was 0.04 cm^2. The current modulation of MBOT was measured by a semiconductor parameter analyzer (Agilent Technologies, 4155C) in the glove box, where concentrations of oxygen and water were less than

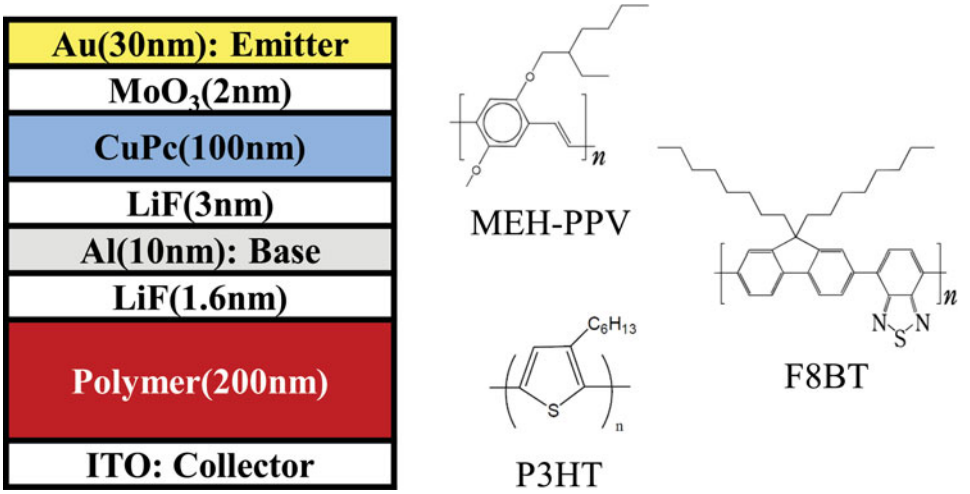

Figure 1. Device structure of the hybrid-type MBOT composed of polymer collector layer and small-molecule emitter layer. The molecular structures of used polymer materials, P3HT, MEH-PPV and F8BT, are also indicated.

1 ppm. The collector voltage (V_C) was applied between the collector and emitter electrodes, and the base voltage (V_B) was applied between the emitter and base electrodes; in both cases, the emitter was positively biased. The current amplification factor (β) is defined as the ratio of the change in the collector current (I_C) to that in the base current (I_B) induced by applying the input voltage (V_B). The energy level of the highest occupied molecular orbital (HOMO) was measured by atmospheric photoelectron spectroscopy (Riken Keiki, AC-3), and the lowest unoccupied molecular orbital (LUMO) was calculated from the band gap estimated from UV/vis absorption spectrum measured by spectrophotometer (JASCO, V-570) of the spin-coated film on a glass substrate.

Result and Discussion

Figure 2 shows the modulation characteristics of three MBOT devices using different materials (P3HT, MEH-PPV, and F8BT) for the collector layer. The output curves (log I_C-V_B) and input curves (log I_B−V_B) at $V_C = -5$V are plotted in the same figure using absolute value. In all devices, the output collector current (I_C) and input base current (I_B) are increased with increasing base voltage (V_B). The device using P3HT for the collector layer [Fig. 2(a)] shows the highest current density among these three devices, where I_C increases abruptly from $V_B = -1.2$ V, and finally reached 12.6 mA/cm^2. The on/off ratio, that is defined as a ratio of I_C at V_B = -3 V and $V_B = 0$ V, exceeds 10^5. In addition, the magnitude of I_B is much smaller than that of I_C. This means that the output current (I_C) is amplified against the input current (I_B). In the case of P3HT, current amplification factor (β) of 76 is achieved at $V_B = -3$ V. In contrast, MEH-PPV [Fig. 2(b)] and F8BT [Fig. 2(c)] show lower I_C. In the case of MEH-PPV, while I_C is increased with increasing V_B, the I_B is higher than the I_C, which means β is less than unity and no amplification. In the case of F8BT, I_C hardly increases with increasing V_B. The I_B is much higher than I_C, resulting in nearly zero of β. The device parameters of the three MBOT devices at $V_C = -5$ V and $V_B = -3$ V are summarized in Table 1. The order of I_C magnitude is P3HT > MEH-PPV > F8BT; in contrast, the order of I_B magnitude is F8BT > MEH-PPV > P3HT. The orders of I_C and I_B are opposite each other.

Figure 3 shows two terminal J-V measurements of three MBOT devices. Fig. 3(a) and Fig. 3(b) show J-V curves of the emitter-base diode and base-collector diode, respectively. In the emitter-base diode, almost similar J-V curves are observed for the three devices having a different collector layer. This result is reasonable because the device structure between the emitter and base electrode is the same (Al/LiF/CuPc/MoO_3/Au); however, it indicates an important fact that the emitter current is not affected by property of the underlayer, such as morphology or hydrophobicity. In the MBOTs, emitter current is directly linked with output current because the output current comes from transmission of the emitter

Table 1. The device performance of the hybrid-type MBOT devices using different collector materials

Collector material	I_C ON (mA/cm^2)	I_B ON (mA/cm^2)	Current amplification:β	On/Off ratio
P3HT	12.6	0.16	76.8	1.5×10^5
MEH-PPV	1.0×10^{-3}	0.28	4.0×10^{-3}	94
F8BT	$1.2 \times 1\,0^{-6}$	1.34	1.2×10^{-6}	0.43

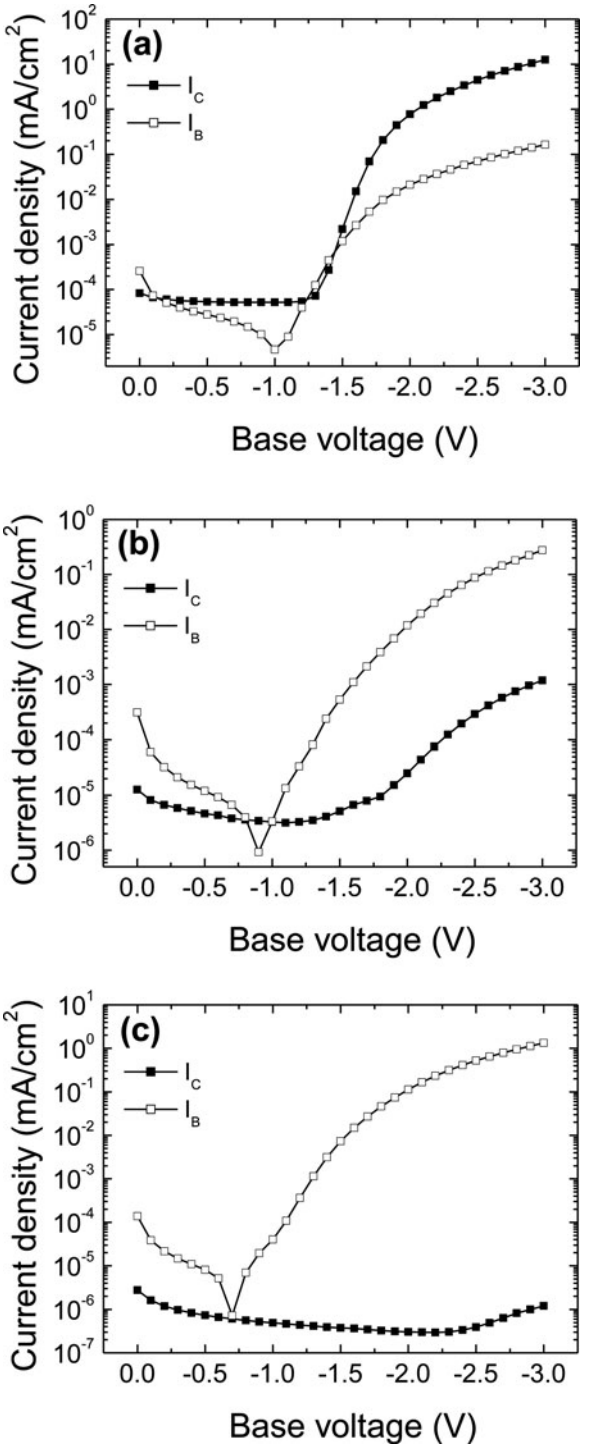

Figure 2. The output curves (I_C-V_B) and input curves (I_B-V_B) at $V_C = -5$ V in three MBOT devices using different materials for the collector layer, (a) P3HT, (b) MEH-PPV, and (c) F8BT.

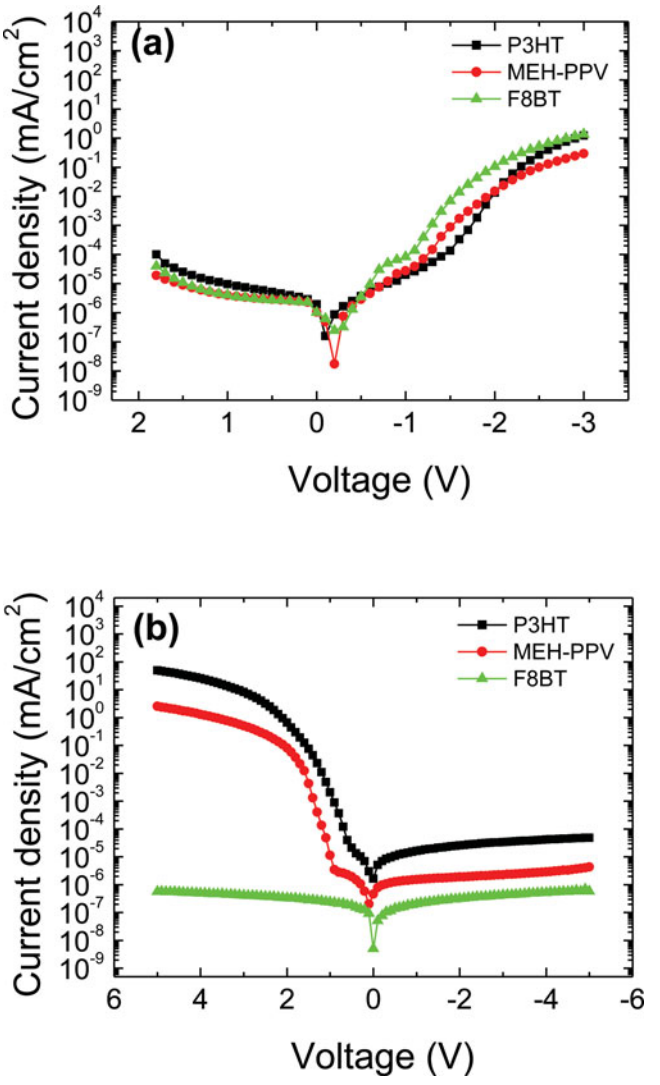

Figure 3. J−V curves of two terminal measurements in the ITO/polymer/LiF/Al/LiF/CuPc/MoO_3/Au devices, (a) the emitter-collector diode, and (b) the base-collector diode.

current. Therefore, the difference of output current as shown in Table 1 should be explained by nature of the collector layer. In fact, the J-V curves of the base-collector diodes are obviously different dependent on the collector materials. The order of current magnitude is P3HT > MEH-PPV > F8BT in both bias polarities. This order can be easily interpreted by HOMO levels (P3HT: 4.8 eV, MEH-PPV: 5.3 eV, F8BT: 6.0 eV). When the collector electrode is positively biased, a large amount of holes are injected from the ITO electrode. In the case of P3HT, a large current around 50 mA/cm^2 is observed at $V_{BC} = 5$ V. In contrast, when the collector electrode is negatively biased, small current (0.05 μA/cm^2 for P3HT) is observed because hole injection from the Al base electrode is difficult. This current component corresponds to "off current" in the MBOT measurement.

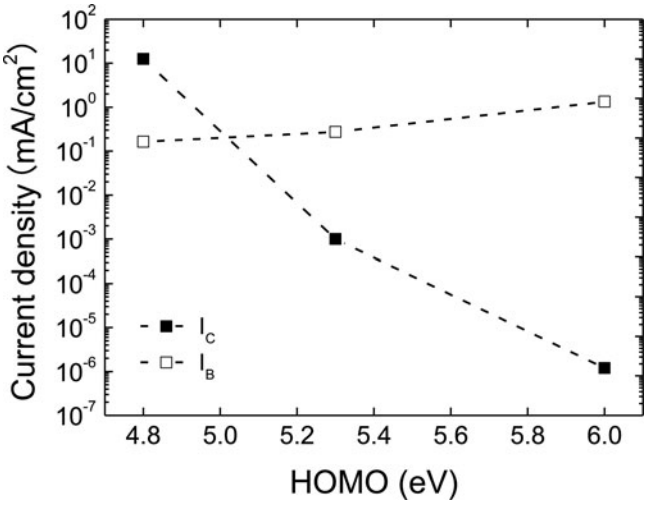

Figure 4. Relationship between the magnitude of collector and base current modulation, and HOMO levels of the collector materials.

The relationship between the magnitude of current and HOMO levels of the collector materials is shown in Fig. 4. The deeper HOMO level of the collector layer brings about steep decrease of I_C and gradual increase of I_B. The intersection point between two lines is around 5.0 eV. As a transistor, current amplification factor must be higher than unity. Therefore, this result means that the material having higher HOMO level than 5.0 eV is suitable for collector layer to achieve current amplification.

The observed results can be explained by energy level diagrams indicating operation mechanism of the MBOT as shown in Fig. 5. For current amplification, the emitter current must be transmitted through the base layer just as it does in silicon bipolar transistors. When emitted holes from the emitter layer transmit through the base layer, they are collected to the collector layer and observed as I_C. In contrast, when the emitted holes cannot be transmitted, they are collected to the base electrode and observed as I_B. In the case of P3HT, the HOMO level of the collector layer is higher than that of CuPc (5.2 eV). The emitted holes from the emitter layer can plunge into the collector layer as shown in Fig. 5(a). Therefore, high I_C and low I_B leading to current amplification are observed. In contrast, the HOMO levels of F8BT and MEH-PPV is lower than that of CuPc. Therefore, emitted holes are blocked by the collector layer at the collector layer / base electrode interface [Fig. 5(b)]. They fall into the base electrode and increase I_B. As a result, low I_C and high I_B, that is, no amplification is observed. From these results, we can conclude that the material having a higher HOMO level compared to that of the emitter layer is suitable for the collector layer in the MBOTs. Conversely, if air-stable polymer having a deep HOMO level is used for the collector layer, it is necessary that the emitter layer material should have a further deeper HOMO level.

Conclusion

In conclusion, the hybrid-type MBOT composed of polymer collector layer and small-molecule based emitter layer was fabricated. The device using P3HT achieved high output current density of 12.6 mA/cm^2 and large current amplification of 76. From dependence of collector materials on the MBOT performance, we obtained an important guideline that

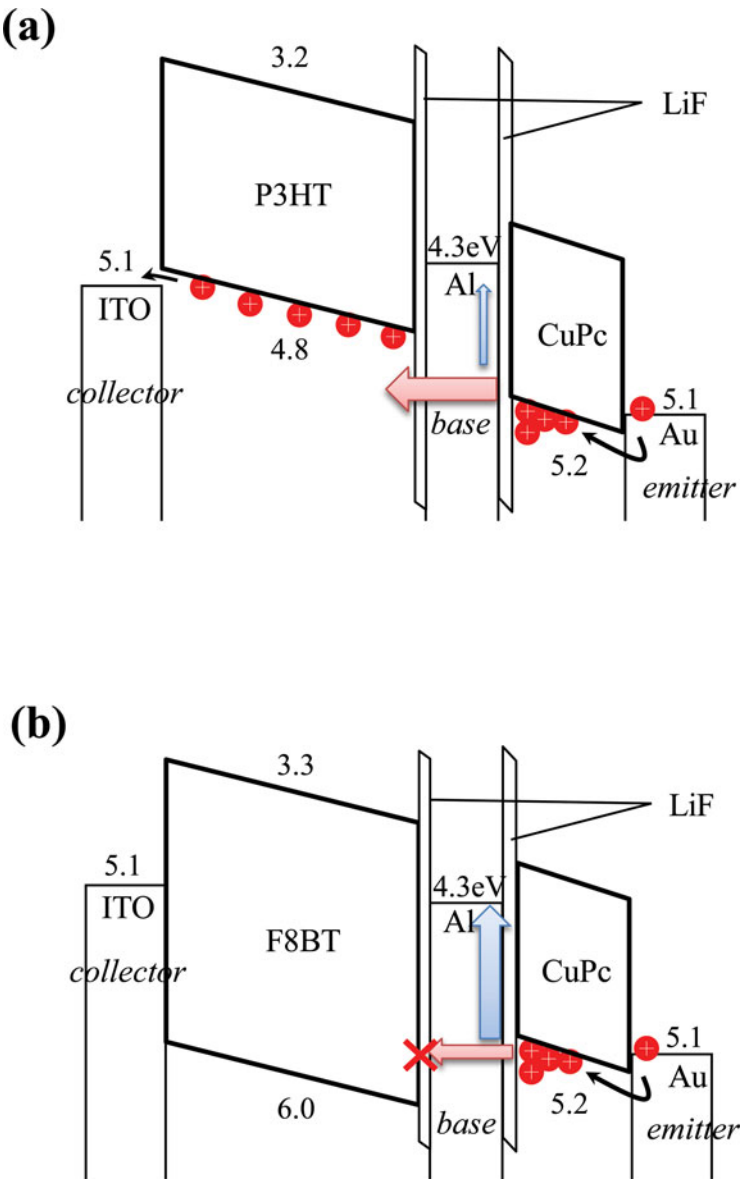

Figure 5. The energy level diagrams for the hybrid MBOT devices using different materials for the collector layer, (a) P3HT, and (b) F8BT.

the collector layer material should have a higher HOMO level than that of the emitter layer material. This guideline would help further work for elucidation of current transmission mechanism and material development for the MBOTs.

Acknowledgments

This research was supported by the New Energy and Industrial Technology Development Organization (NEDO), PRESTO program by the Japan Science and Technology Agency

(JST), a Grant-in-Aid for Scientific Research from the Japan Society for the Promotion of Science (JSPS).

References

[1] Zhou, L. S., Wanga, A., Wu, S. C., Sun, J., Park, S., & Jackson, T. N. (2006). *Appl. Phys. Lett.*, *88*, 083502.
[2] Sekitani, T., Nakajima, H., Maeda, H., Fukushima, T., Aida, T., Hata, K., & Someya, T. (2009). *Nat. Mater.*, *8*, 494.
[3] Cantatore, E., Geuns, T. C. T., Gelinck, G. H., Van Veenendaal, E., Gruijthuijsen, A. F. A., Schrijnemakers, L., Drews, S., & De Leeuw, D. M. (2007). *IEEE J. Solid-State Circuits*., *42*, 84.
[4] Myny, K., Steudel, S., Smout, S., Vicca, P., Furthner, F., Van der Putten, B., Tripathi, A. K., Gelinck, G. H., Genoe, J., Dehaene, W., & Heremans, P. (2011). *Org. Electron*., *11*, 1176.
[5] Kudo, K., Wang, D. X., Iizuka, M., Kuniyoshi, S., & Tanaka, K. (1998). *Thin Solid Films*, *331*, 51.
[6] Watanabe, Y., Iechi, H., & Kudo, K. (2006). *Appl. Phys. Lett*., *89*, 233509.
[7] Fujimoto, K., Hiroi, T., Kudo, K., & Nakamura, M. (2007). *Adv. Mater.*, *19*, 525.
[8] Chao, Y. C., Meng, H. F., & Horng, S. F. (2008). *Appl. Phys. Lett*., *88*.
[9] Chao, Y. C., Meng, H. F., Horng, S. F., & Hsu, C. S. (2008). *Org. Electron*., *9*, 310.
[10] Chao, Y. C., Lin, Y. C., Dai, M. Z., Zan, H. W., & Meng, H. F. (2009). *Appl. Phys. Lett*., *95*, 203305.
[11] Chao, Y. C., Yang, S. L., Meng, H. F., & Horng, S. F. (2005). *Appl. Phys. Lett*., *87*, 253508.
[12] Chao, Y. C., Xie, M. H., Dai, M. Z., Meng, H. F., Horng, S. F., & Hsu, C. S. (2008). *Appl. Phys. Lett*., *92*, 093310.
[13] Ou, T. M., Cheng, S. S., Huang, C. Y., Wu, M. C., Chan, I. M., Lin, S. Y., Chan, Y. J. (2006). *Appl. Phys. Lett*., *89*, 183508.
[14] Cheng, S. S., Yang, C. Y., Chuang, Y. C., Ou, C. W., Wu, M. C., Lin, S. Y., & Chan, Y. J. (2007). *Appl. Phys. Lett*., *90*, 153509.
[15] Cheng, S. S., Chen, J. H., Chen, G. Y., Kekuda, D., Wu, M. C., & Chu C. W. (2009). *Org. Electron*., *10*, 1636.
[16] Huang, J. Y., Yi, M. D., Ma, D. G., & Hummelgen, I. A. (2008). *Appl. Phys. Lett*., *92*, 232111.
[17] Yi, M. D., Huang, J. Y., Ma, D., & Hummelgen, I. A. (2008). *Org. Electron*., *9*, 539.
[18] Fujimoto, S., Nakayama, K., & Yokoyama, M. (2005). *Appl. Phys. Lett*., *87*, 133503.
[19] Nakayama, K., Fujimoto, S., & Yokoyama, M. (2006). *Appl. Phys. Lett*., *88*, 153512.
[20] Nakayama, K., Fujimoto, S., & Yokoyama, M. (2009). *Org. Electron*., *10*, 543.
[21] Suzuki, F., Nakayama, K., Pu, Y. J., Yokoyama, M., & Kido, J. (2010). *Jpn. J. Appl. Phys*., *49*, 030202.
[22] Nakayama, K., Akiba, R., & Kido, J. (2012). *Appl. Phys. Express*., *5*, 094202.